WOODS HOLE OCEANOGRAPHIC INSTITUTION

REFERENCE NO. 68-56

MOLECULAR STRUCTURE AND COMPOSITION OF FISH OTOLITHS

by

Egon T. Degens, Werner G. Deuser
and Richard L. Haedrich

GPO PRICE $ _____

CSFTI PRICE(S) $ _____

Hard copy (HC) ____

Microfiche (MF) _____

ff 653 July 65

WOODS HOLE, MASSACHUSETTS

WOODS HOLE OCEANOGRAPHIC INSTITUTION
Woods Hole, Massachusetts

REFERENCE NO. 68-56

MOLECULAR STRUCTURE AND COMPOSITION OF FISH OTOLITHS

by

Egon T. Degens, Werner G. Deuser
and Richard L. Haedrich

August 1968

TECHNICAL REPORT

Submitted to the National Aeronautics and Space Administration under Contract NSR-22-014-001; with the American Chemical Society Grant PRF 1943A2; and with the National Science Foundation Grant GA-970.

Approved for Distribution

J. M. Hunt, Chairman
Department of Chemistry

Abstract

Recent and fossil otoliths from 25 different fishes have been studied for their amino acid content and for their C^{13}/C^{12} and O^{18}/O^{16} distribution in the carbonate fraction. The selection includes specimens from a wide phylogenetic range as well as from various fresh water and marine habitats.

All otoliths are composed of aragonite, and their total organic matter ranges from 0.2 to 10 percent. The organic matter is a protein (MW $>$ 150,000), which is characterized by a high abundance of acidic amino acids. In comparison to molluscs that exhibit a wide variety of different mineralized tissues which are species specific, the proteinaceous matter of all otoliths is chemically rather uniform.

The high abundance of oxygen-rich amino acids accounts for the ease of mineralization of the organic template. Namely, oxygen supplied by carboxyl groups is used for the coordination of Ca^{++} ions, resulting in the formation of metal ion coordination polyhedra. Carbonate groups linked via hydrogen bridges to the template will exchange their oxygen with that of the metal polyhedra to stabilize the structure; $Ca^{++}O_9$ polyhedra are the consequence. Subsequent nucleation and crystal growth will lead to aragonite.

Oxygen and carbon isotope data indicate that the aragonite is formed close to isotopic equilibrium with the sea. This is surprising because sea water has no direct access to the inner ear where the otolith originates. Isotope data may serve a threefold purpose: (1) to determine the mean water temperature where the fish lived, (2) to distinguish between fresh water and marine fish in ancient deposits, and (3) to reveal information on migratory tendencies of fish.

Introduction

Collagen and phosphates are the principal constituents of vertebrate bones, scales, and teeth. The structural interrelationship between the organic and inorganic phase suggests that collagen acts as a template in the nucleation of apatite crystals (e.g., Glimcher, 1960). In addition to bones, scales, and teeth, fishes deposit otoliths in their inner ear (Figs. 1 and 2). These are small carbonate stones, a few milligrams to grams by weight, which morphologically and sizewise are species specific (e.g., Sanz-Echeverria, 1949). Little is known, however, regarding their mode of formation, chemical nature, and physiological function.

As part of a program on origin and evolution of mineralized tissues, we collected a series of 25 otoliths of fishes of wide phylogenetic range from fresh water and marine habitats. One fossil otolith of Miocene age (ca. 25 million years) was included in the selection in order to study diagenetic effects.

The present work is principally concerned with

(a) mineralization processes leading to otoliths,

(b) phylogenetic implications in terms of evolutionary trends, and

(c) the possible physiological significance of otoliths per se.

A wide array of analytical tools was employed including X-ray diffraction analysis, optical microscopy, electron microscopy, various chromatographic techniques for the identification of organic matter contained in otoliths, and stable isotope mass spectrometry.

Results

X-ray diffraction data indicate that all specimens are monomineralic and composed of aragonite. This is also true for the Miocene teleost otolith. This contrasts the observation of Devereux (1967) who reports only calcite from a number of otoliths from the Australian region and from fossil deposits. Yet, his specimens are related at the family level to some of the Atlantic otolith samples reported here.

Thin sections parallel and perpendicular to the lenticular faces (Figs. 3 and 4) reveal dark brown bands that run approximately parallel to the outer surface of the otolith. They represent growth rings of apparently organic material. The aragonite crystals are oriented with their c axis perpendicular to the bands or their projected surfaces, respectively. They run from the center to the margin of the otolith without being physically interrupted by the band pattern. As a general rule the spacing of the concentric rings that can be resolved by optical microscopy widens towards the margin. In addition, the frequency of bands is less for larger otoliths when compared to the smaller varieties. A band pattern of this kind is analogous to that observed in fish scales. This feature is commonly interpreted to represent annual or seasonal growth rings which allow the age dating of fish.

A set of electron micrographs delineates in detail the fabric of the otoliths. Rather striking is (a) the intergrowth of aragonite fibrils giving rise to a zig-zag pattern (Fig. 5), and (b) the twinning of individual crystals (Fig. 6). In both pictures the incremental growth along the c axis is well documented. As a

conservative estimate, three to five growth interruptions per micron are observed for Aplidonotus (Fig. 5), whereas ten to fifteen interruptions per micron occur with Roccus (Fig. 6). The Aplidonotus otolith is about three times the size of that of Roccus; the same relations exist for the individual aragonite needles which measure between 2 and 4 millimeters for Aplidonotus. In turn, each aragonite crystal is composed of about 5,000 to 10,000 individual growth segments.

Bands transverse to c as well as the twinning of aragonite can be recognized in Figure 7. These bands have the appearance of sutures, but they do not interfere with the oriented growth of the single crystals. The bands are spaced a few microns apart, and the general position of the micrograph is close to the center of the otolith. As can be judged from the shadow pattern (Fig. 8), a section perpendicular to c exposes the surface of the bands. The bands must represent rather thin films because the structural pattern of the aragonite needles can still be recognized beneath the outer rim of the upper band which actually is flapped over. Also note the virtual disappearance of the lower band when approaching the margin of the picture due to the less favorable breaking and separation of the aragonite bundles during the preparation of the specimen.

The following two electron micrographs (Figs. 9 and 10) show the surface of the organic template in great detail. Again the aragonite structure shines through the organic film (Fig. 9; lower right corner) and the growth pattern of the organic matrix becomes evident. The fibrous material is oriented in a kind of corrugated pattern with well defined lineages and the individual chains are organized in a helical fashion. At certain intervals, the chains are twisted to such an extent that

lumps or knots of "apparently tangled" fibers appear about 0.1 to 0.3 μ apart. The cross section of an individual fiber which measures about 100 Å shows an internal structure; the resolution of this picture, however, is not sufficient to permit a further elaboration as to the nature of this structure. Magnifications up to 750,000 times have been made which reveal ultra structures at the 20 Å level (in preparation).

The organic template in otoliths is a protein with a molecular weight greater than 150,000 as ascertained by molecular sieve techniques. A urea/hydroxylamine treatment (Degens et al., 1967a) will degrade the proteins to units of 70,000 to 80,000 MW. The amino acid analysis, following a technique by Degens et al. (1967b), is rather uniform for all otoliths investigated (Table 1), and the urea/hydroxylamine treated fraction has an identical amino acid distribution as the undegraded material. It is concluded that we are dealing with a new type of fibrous protein which has not been previously described. This protein is characterized by the high abundance of aspartic and glutamic acids, the presence of cystine and hydroxyproline and a low content in aromatic and basic amino acids. The total yield in organic matter fluctuates strongly among otoliths from different species with a range between 0.2 and 10 percent of the total. If weight is used as a measure of size and thickness of otoliths (Sanz-Echeverria, 1949), the specimens that contain the highest amount of organic matter are generally the smallest or thinnest.

The distribution of carbon and oxygen isotopes in the carbonate material is similar to that commonly observed in marine and fresh water shell materials, for

instance, in molluscs, foraminifera, and coccoliths. The data (Table 2) are reported in terms of per mil deviation relative to the PDB standard (Craig, 1957):

$$\delta C^{13} = \left(\frac{R}{R_{standard}} - 1\right) \cdot 1{,}000$$

where $R = C^{13}/C^{12}$ ratio in the sample, and $R_{standard} = C^{13}/C12$ ratio in the standard. δO^{18} is defined similarly in terms of O^{18}/O^{16} ratio.

The most interesting aspect of the isotope data are the δC^{13} values which show a certain environmental (fresh water versus marine) and phylogenetic trend. In any event, however, most of the carbon laid down as carbonate has been derived from sea water or fresh water bicarbonate and not -- as was initially expected on biological grounds -- from respiratory CO_2. Analogously, the oxygen in the carbonate is deposited in isotopic equilibrium with its surrounding environment which in turn permits the calculation of the average water temperature at which the fish lived, as has already been stated by Devereux (1967).

Discussion and Conclusions

In contrast to invertebrates with their species-specific shell organic matrix (Degens et al., 1967b), fishes secrete a distinct but uniform protein for the otolith formation. In this way they follow the same conservative pattern set by collagen with respect to bone, scale, or dentine deposition. Nevertheless, a certain spread in the concentration of amino acids can be recognized (Table 1) which particularly concerns hydroxyproline, proline, serine, and the acidic amino acids. However, these

variations can be considered minor in view of the wide phylogenetic and environmental range of the otolith specimens studied (Fig. 11). This characteristic is somewhat comparable to collagen where the amino acid distribution also varies within certain limits among species of wide phylogenetic range (Table 3).

In summary, the high-molecular-weight fibrous protein (> 150,000 MW) in otoliths is not affected at the molecular level by environmental or phylogenetic events. It is uniform in composition and structurally well-defined. To emphasize its functional and structural significance in the formation of otoliths, the term otolin is proposed for this protein.

Chemically, otolin resembles keratin in the relative abundances of threonine, glycine, valine, methionine, the leucines, lysine and histidine. The presence of cystine underlines this relationship. It shares with collagen the presence of hydroxyproline, the low abundance of aromatic amino acids, and about the same level in alanine, serine, lysine and histidine. The low content in basic amino acids, in particular arginine, is noteworthy. Actually, the small amount in basic amimo acids is a general feature of all fibrous proteins.

This type of relationship may suggest that all fibrous proteins have a common ancestor. To test this assumption all codon assignments for an individual amino acid were given equal weight. To find common denominators for the various fibrous proteins, a computer program was worked out (Spencer and Degens, 1969). The solution involved codon-anticodon relationships and the base substitution one at a time. For example, the substitution of C_{II} codons in the glycine triplets

(i.e. guanine vs. adenine) will result in the formation of the aspartic acid (GAU and GAC) and glutamic acid (GAA and GAG) codon assignments. Interestingly, the sum of glutamic acid, aspartic acid and glycine is about the same for otolin and collagen. If we take the anticodons of glycine, the assignments read proline; the anticodons for aspartic and glutamic acid will yield four of the leucine triplets. Glycine and proline (+hydroxyproline), and the acidic amino acids and leucine appear to go along in both collagen and otolin. There are, of course, many thousands of different solutions conceivable; yet the computer program will select the most probable ones and discriminate against the others.

The actual mineralization of otolin is a dual process:

In the first place, metal ions become coordinated to oxygens displayed at the surface of otolin. Like hydrogen bonds, these metal ion bridges give the protein a higher biocrystallographical order by forming metal ion coordination polyhedra (Matheja and Degens, 1968). The high abundance of oxygen functions will promote the formation of $Ca^{++}O_9$ polyhedra. Bicarbonate can be linked via hydrogen bridges to a number of amino acids.

In the second place, oxygen substitution at the polyhedra will take place allowing the oxygens of the bicarbonate to participate in the polyhedra structure. This will result in a more stable conformation and nucleation is initiated. Inasmuch as $Ca^{++}O_9$ polyhedra and not $Ca^{++}O_6$ polyhedra are present, aragonite and not calcite will be the mineral form.

The incremental growth pattern of the aragonite (Figs. 5 and 6) could be explained if we assume that nucleation sites of calcite ($Ca^{++}O_6$) sporadically

interfere with aragonite growth. No indication for the presence even of traces of calcite can be found on the X-ray diagrams. The observation of Morris and Kittleman (1967) concerning the presence of sodium in otoliths in concentrations of about 2 mole percent relative to calcium (=100) is rather significant. At this scale, isomorphous substitution of sodium for calcium in aragonite is rather unlikely. Morris and Kittleman (1967) tentatively suggested the presence of minerals such as shortite $Na_2Ca_2(CO_3)_3$ or pirssonite $Na_2Ca(CO_3)_2 \cdot 2\,H_2O$. Both minerals are orthorhombic, as is aragonite. Wedge-shaped crystals are the typical habitus of shortite.

X-ray diffraction analysis shows no reflections at the proper spacings for shortite and pirssonite except for peaks that coincide with aragonite. However, to be detected by this technique, mineral concentrations of a few percent are required. Inasmuch as sodium does not proxy for calcium in the aragonite lattice at the level found in otoliths, it can only be accounted for as a trace mineral unless we assume that sodium occupies coordination sites within the organic matter causing the formation of oxygen coordination polyhedra. In both instances sodium ions will interfere with the growth of aragonite and epitaxial growths of the type observed in some of the electronmicrographs are the consequence. We suspect that, in some way, the Ca/Na ratio of otoliths is related to the number of wedges in the aragonite crystals, the total organic matter, and the weight and size of the otolith.

The interpretation of the stable isotope data requires a reassessment of the biological record. The inner ear of sharks is open to the sea whereas the inner ear

of bony fishes forms a closed membranous labyrinth filled with endolymph (Fig. 1). Yet, the carbon isotope pattern of the aragonites in marine otoliths clearly indicates that most if not all carbon is directly derived from sea water bicarbonate. Respiratory CO_2 has a δC^{13} near that of most marine organisms (-15 to -20 per mil). We thus have to assume that sea water can enter freely, or via permeable membranes, the inner ear canals and deposit calcium carbonate in the form of otoliths. In those instances where the δC^{13} values are slightly negative, for instance, in Ariomma or Nomeus, small contributions of respiratory CO_2 might be anticipated. It is interesting to note (Table 2) that certain phylogenetic trends become apparent. All marine Paracanthopterygii have δC^{13} values like sea water bicarbonate. In contrast, the highly advanced marine Acanthopterygii have a range in δC^{13} between -4 and -5 per mil. The most likely explanation for the phylogenetic differences in δC^{13} is probably related to the more effective passage of sea water bicarbonate into the inner ear of the Paracanthopterygii in compraison to the highly evolved Acanthopterygii. As a consequence, contributions from respiratory CO_2 may play a more important role in the case of the Acanthopterygii. Perhaps the larger size of Paracanthopterygii otoliths and their low organic matter content is a reflection of this phenomenon. The fresh water forms are depleted in C^{13} by about 10 per mil which corresponds exactly to the mean difference in δC^{13} between fresh water and marine dissolved carbonate.

The oxygen in marine otoliths is deposited in isotopic equilibrium with the sea. This allows the determination of the water temperature at which the fish lived. There is good agreement between the calculated isotopic temperature and the water

temperature at the time the fish was collected. Analogously, fresh water otoliths are deposited in isotopic equilibrium with river or lake waters which commonly are about 10 per mil depleted in O^{18} relative to the ocean. This feature may be used to determine migratory tendencies of fish. For instance, in the present set of samples Osmerus is known to enter fresh water habitats. Its δO^{18} (Table 2) is slightly lower than one would expect if Osmerus had deposited its otoliths exclusively in a marine environment; but more data are required to substantiate this relationship.

Questions on the physiological function of otoliths have recently been touched upon by Morris and Kittleman (1967). The fact that otoliths exhibit piezoelectric properties suggested to them that here, in theory, a mechanism for depth perception or frequency analysis of sound waves is conceivable. The Parophrys otolith oscillated from as low as 1 to 15,000 cycle/sec. Multicrystalline structures, such as bones, show piezoelectric effects (Shamos et al., 1963); so do soft biological tissues (Shamos and Lavine, 1967). Among the piezoelectric minerals that respond to hydrostatic pressure and compression and torsion are shortite and pirssonite (Giebe and Scheibe, 1925).

In conclusion, the epitaxial relationships between organic matter and minerals and the wedge-shaped pattern of the aragonite crystals in otoliths suggest that this fabric functions as a piezoelectric body and that this property is used by fishes in the manner suggested by Morris and Kittleman (1967).

Diagenesis leaves a significant imprint on the organic matter of otoliths. The marine teleost otolith of Miocene age is morphologically similar to Gadus

and Melanogramus. The total organic matter in the Miocene specimen, however, is only about a third to a fourth that of its suggested recent counterpart. Best preserved among the amino acids are alanine, cystine, proline, valine and glutamic acid, whereas aspartic acid, serine, threonine and hydroxyproline have suffered the greatest losses (Table 1). This phenomenon is a result of the structural organization of otolin which contains a stable core of selected amino acids among which alanine and cystine are the most outstanding members. The band pattern and the orientation of the aragonite fibrils is still intact. The stable isotope distribution ($\delta O^{18} = +2.5$ and $\delta C^{13} = +0.4$ per mil) is preserved indicating that the fish lived at water temperatures of around 7°C.

Summary

1. Otoliths are mineralogically composed of aragonite. The aragonite fibrils are arranged with their long axis about perpendicular to the outer margin of the otoliths. Bands of organic matter intersect the aragonite fibrils transverse to c; the spacing of the bands narrows towards the center of the otoliths.

2. The interrelationship between organic and inorganic matter indicates that the aragonite is formed by epitaxial growth on a protein matrix. Metal ions become coordinated to the oxygen functions displayed on the organic tissue, resulting in the formation of metal ion coordination polyhedra, and bicarbonate becomes linked via hydrogen bridges to amino acids. Subsequent exchange of bicarbonate oxygen for metal ion polyhedra oxygen will stabilize the structure and introduce

the nucleation of mineral seeds. Inasmuch as $Ca^{++}O_9$ polyhedra are involved, the mineral form will be aragonite.

3. The mineralized tissue is a fibrous protein with a molecular weight exceeding 150,000. The amino acid composition is biochemically unique and not affected by phylogenetic and environmental events. The term otolin is proposed for this new kind of protein.

4. The variation of total organic matter and the stable isotope distribution in the aragonite can be used as phylogenetic and environmental criteria to distinguish, for example, between fresh water and marine species, to determine migratory tendencies, or to measure the mean temperature at which the fish lived.

5. The compositional variation of otoliths in combination with their ultrastructure suggests that otoliths may function as piezoelectric body for the recording of depth and sound.

Acknowledgements

We are grateful to Mr. J. C. Hathaway for the X-ray analyses and to Mr. J. B. Waterbury for assistance in the electronmicroscopy. Some of the otolith specimens were kindly made available to us by Dr. Johanna Rinehart and Mr. A. Konnerth, Jr. The work was supported by the National Aeronautics and Space Administration Project NSR-22-014-001, the Petroleum Research Fund Project PRF-1943-A2, administered by the American Chemical Society, and by the National Science Foundation Contract GA 970.

Literature Cited

Craig, H. : Isotopic standards for carbon and oxygen and correction factors for mass-spectrometric analysis of carbon dioxide. Geochim et Cosmochim. Acta 12, 133-149 (1957).

Degens, E. T., B. W. Johannesson, and R. W. Meyer : Mineralization processes in molluscs and their paleontological significance. Naturwissenschaften 54, 638-640 (1967a).

Degens, E. T., D. W. Spencer, and R. H. Parker : Paleobiochemistry of molluscan shell proteins. Comp. Biochem. Physiol. 20, 533-579 (1967b).

Devereux, I. : Temperature measurements from oxygen isotope ratios of fish otoliths. Science 155, 1684-1685 (1967).

Giebe, E., and A. Scheibe : Eine einfache Methode zum qualitativen Nachweis der Piezoelektrizität von Kristallen. Ztschr. Physik 33, 760-766 (1925).

Glimcher, M. J. : Specificity of the molecular structure of organic matrices in mineralization. Amer. Assoc. Adv. Sci. Publ. No. 64, 421-487 (1960).

Greenwood, P. H., D. E. Rosen, S. H. Weitzman, and G. S. Myers : Phyletic studies of teleostean fishes, with a provisional classification of living forms. Bull. Amer. Mus. Nat. Hist. 131, 339-456 (1966).

Matheja, J., and E. T. Degens : Molekulare Entwicklung mineralisationsfähiger organischer Matrizen. N. Jb. Geol. Paläont. Mh. 1968, 215-229 (1968).

Morris, R. W., and L. R. Kittleman: Piezoelectric property of otoliths. Science 158, 368-370 (1967).

Sanz-Echeverria, J. : Identificación de los peces de la familia Centrolophidae de España por medio de los otolitos. Real Soc. Esp. Hist. Nat. Tomo. Extraordinaire, 151-156 (1949).

Shamos, M. H., and L. S. Lavine : Piezoelectricity as a fundamental property of biological tissue. Nature 213, 267-269 (1967).

Shamos, M. H., L. S. Lavine, and M. I. Shamos : Piezoelectric effect in bone. Nature 197, p. 81 (1963).

Spencer, D. W., and E. T. Degens : (unpublished results).

TABLE I

DISTRIBUTION OF AMINO ACIDS IN OTOLITHS

(in residues per 1000)

	OH-PRO	ASP	THR	SER	GLU	PRO	GLY	ALA	CYS	VAL	MET	ILEU	LEU	TYR	PHE	LYS	HIS	ARG	Total %
								MARINE											
Melanogramus aeglefinus	33	125	74	51	132	99	141	87	12	77	1	24	91	tr.	17	18	7	13	0.25
Gadus callarias	48	122	68	68	115	101	143	83	13	87	1	19	79	tr.	15	19	7	13	0.29
Psenopsis obscura	27	168	76	106	150	29	95	90	19	71	1	37	85	tr.	7	18	7	14	0.46
Ceratoscopelus maderensis	30	171	77	92	149	49	126	100	19	68	1	18	45	tr.	10	19	9	19	0.48
Merluccius bilinearis	28	151	58	27	192	48	130	96	14	92	1	32	97	tr.	13	11	4	7	0.53
Centrolophus niger	49	170	49	40	159	56	132	104	16	70	1	30	76	tr.	7	24	7	11	0.71
Prionotus evolans	21	125	72	82	159	56	137	81	34	76	1	33	77	1	11	19	5	9	0.64
Prionotus evolans	29	146	64	49	170	47	144	111	32	67	1	27	66	tr.	16	18	4	9	0.84
Peprilus triacanthus	22	173	49	25	165	33	110	104	28	76	1	36	78	tr.	6	52	15	28	0.86
Stenotomus versicolor	11	181	59	24	202	39	106	104	32	76	1	32	76	tr.	20	19	6	13	0.88
Hyperoglyphe bythites	19	167	67	97	167	36	124	103	15	68	1	29	66	tr.	9	14	6	12	0.91
Pomatomus saltatrix	19	144	68	117	137	57	129	94	13	72	1	32	69	3	8	19	7	14	1.03
Cubiceps sp.	67	186	42	36	170	96	85	78	15	69	1	33	62	tr.	8	25	9	19	1.04
Roccus lineatus	18	131	66	114	134	52	144	88	11	56	1	29	67	2	7	43	18	19	1.19
Seriolella violacea	35	185	54	27	161	53	164	106	19	43	1	28	68	tr.	15	24	6	13	1.28
Osmerus mordax	45	112	44	43	157	74	196	95	10	49	1	28	67	tr.	14	29	12	23	1.38
Stromateus stellatus	34	190	52	35	182	47	124	94	15	68	1	31	67	tr.	17	22	6	14	1.65
Pomolobus pseudoharengus	22	184	49	36	191	32	111	117	25	82	1	32	66	tr.	8	22	8	16	1.76
Pampus argenteus	23	172	69	95	151	37	125	84	16	64	1	36	68	1	12	22	9	18	1.84
Schedophilus pemarco	26	175	62	72	173	46	115	91	12	62	1	36	70	tr.	14	21	6	17	3.22
Ariomma regulus	37	181	48	30	182	42	124	89	12	67	1	38	95	tr.	11	20	8	15	4.31
Nomeus gronowi	25	169	47	31	220	40	115	86	13	78	1	45	79	tr.	21	13	4	14	10.14
MEAN	32	162	60	60	168	53	126	94	19	69	1	30	71	1	12	22	8	15	
								FRESH WATER											
Aplodinotus grunniens	9	223	82	87	169	45	98	81	9	46	1	29	48	3	13	25	12	22	0.32
Lota maculosa	7	133	63	97	174	94	116	88	33	65	tr.	15	57	1	12	29	4	14	0.59
MEAN	8	178	73	92	172	70	107	85	21	56	1	22	53	2	13	27	8	18	
								FOSSIL (MARINE)											
Teleost	--	22	6	11	213	109	51	303	100	134	--	19	34	--	--	n.d.	n.d.	n.d.	0.081

TABLE 2

PHYLOGENETIC RELATIONSHIP* AND ANALYTICAL DATA ON STABLE ISOTOPE DISTRIBUTION AND TOTAL ORGANIC MATTER

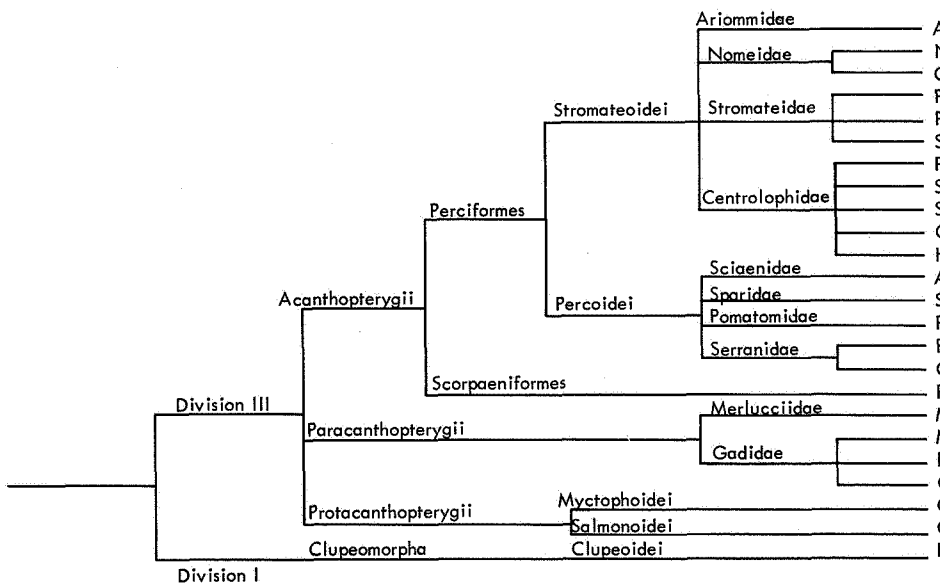

	δC^{13}	% organic	δO^{18}	Calculated O^{18}/O^{16} Temperature °C
Ariomma	-5.5	4.31	+0.8	14 (17)**
Nomeus	-4.6	10.14	-0.1	17
Cubiceps	-4.5	1.04	0.0	16 (11)
Pampus	-4.0	1.84	+0.2	16
Peprilus	-4.6	0.86	-1.1	21
Stromateus	-0.8	1.65	+0.9	13
Psenopsis	-0.9	0.46	+1.1	12 (11)
Seriolella	-0.6	1.28	+1.0	13
Schedophilus	-3.6	3.22	-0.1	17
Centrolophus	-3.2	0.71	+1.3	11
Hyperoglyphe	-1.2	0.91	-0.2	17
Aplodinotus (FW)	-13.1	0.32	-8.1	n.d.
Stenotomus	-4.9	0.88	-1.8	24
Pomatomus		1.03		
Roccus		1.19		
Centropristes	-0.8	n.d.	+0.1	16
Prionotus	-0.2	0.84	-0.2	17
Merluccius	-0.8	0.53	+1.4	11
Melanogramus	+0.5	0.25	+1.5	8
Lota (FW)	-11.0	0.59	-9.6	n.d.
Gadus	+0.3	0.29	+1.9	9
Ceratoscopelus	-4.1	0.48	+2.0	9
Osmerus	-2.5	1.38	-1.5	23
Pomolobus		1.76		

* after Greenwood et al., 1966

** water temperature at time of collection

TABLE 3. GEOMETRIC MEANS OF AMINO ACID IN MINERALIZED AND UNMINERALIZED TISSUES (in residues per 1000)

	OTOLIN	DENTINE				UNMINERALIZED TISSUES				
	Pisces	Elasmo-branchii	Pisces	Reptilia	Mammalia	Collagen	Kera-tin	Fibrinogen	Elastin	Resilin
	(25)*	(9)	(4)	(7)	(10)	(5)	(5)	(5)	(3)	(3)
OH-PRO	30	65	72	82	94	82	—	—	18	—
ASP	162	84	75	60	62	49	65	33	17	101
THR	57	21	27	23	20	21	58	15	13	31
SER	44	50	55	50	41	44	103	131	11	80
GLU	170	60	80	84	81	74	111	18	46	48
PRO	50	101	104	123	124	120	75	7	129	79
GLY	125	354	330	325	324	325	84	292	158	383
ALA	96	112	106	109	105	113	54	281	151	107
CYS (half)	17	2	0.3	0.3	0.3	—	114	—	—	—
VAL	70	27	20	18	20	20	68	24	159	28
MET	0.3	3	4	1	1	6	0.1	—	2	—
I-LEU	30	20	10	12	9	12	34	12	36	17
LEU	73	25	24	24	27	26	74	13	99	23
TYR	<1	1	2	1	2	3	25	46	34	27
PHE	12	5	8	10	9	14	26	5	77	26
OH-LYS	—	5	8	5	7	7	—	—	—	—
LYS	20	14	18	17	17	25	23	7	12	6
HIS	7	3	5	2	2	5	6	3	2	9
ARG	14	35	40	49	45	48	59	24	20	35

* number of analyses

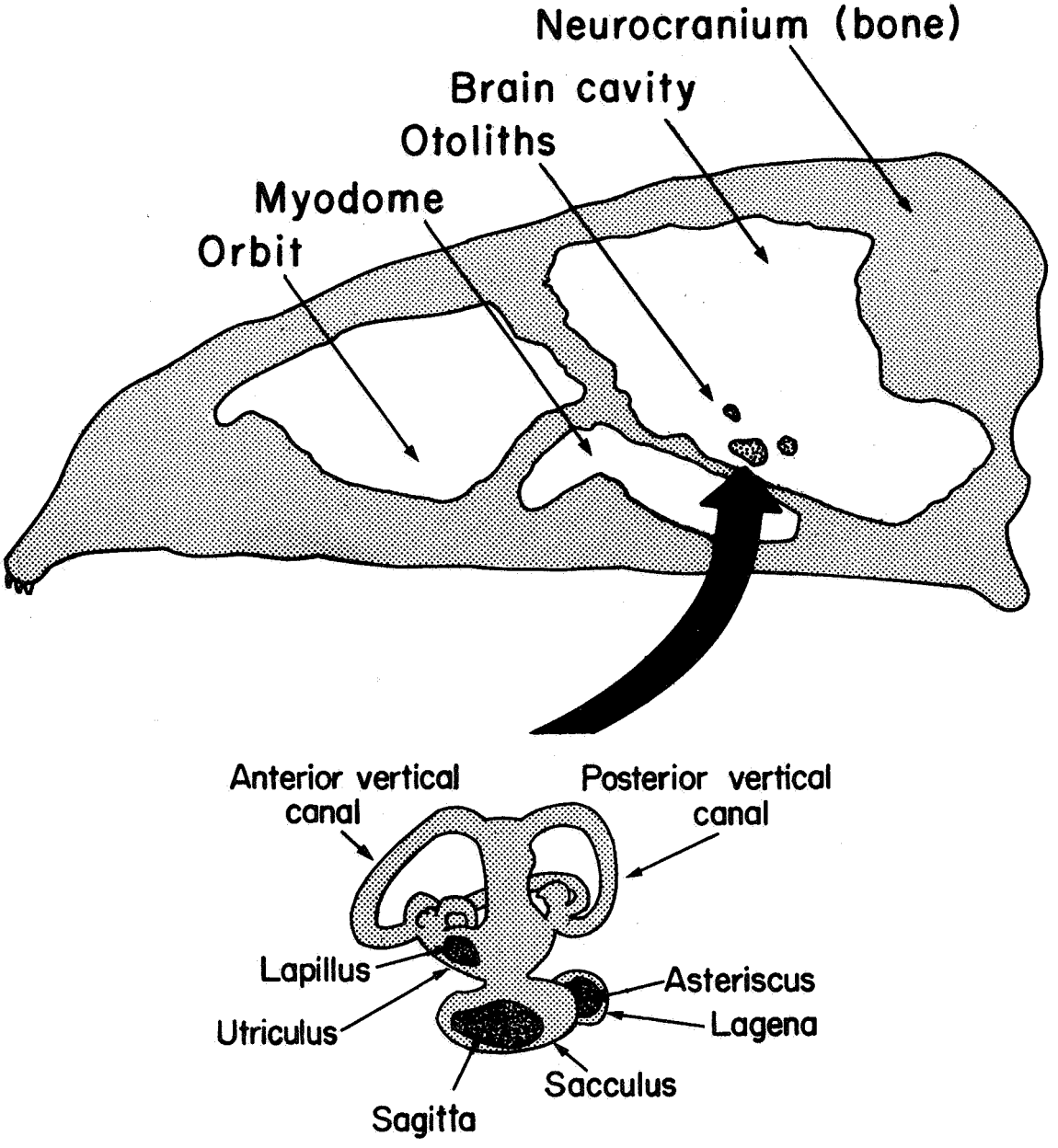

Figure 1

Diagrammatic drawing of the skull of bony fishes with special reference to the location of otoliths in the inner ear.

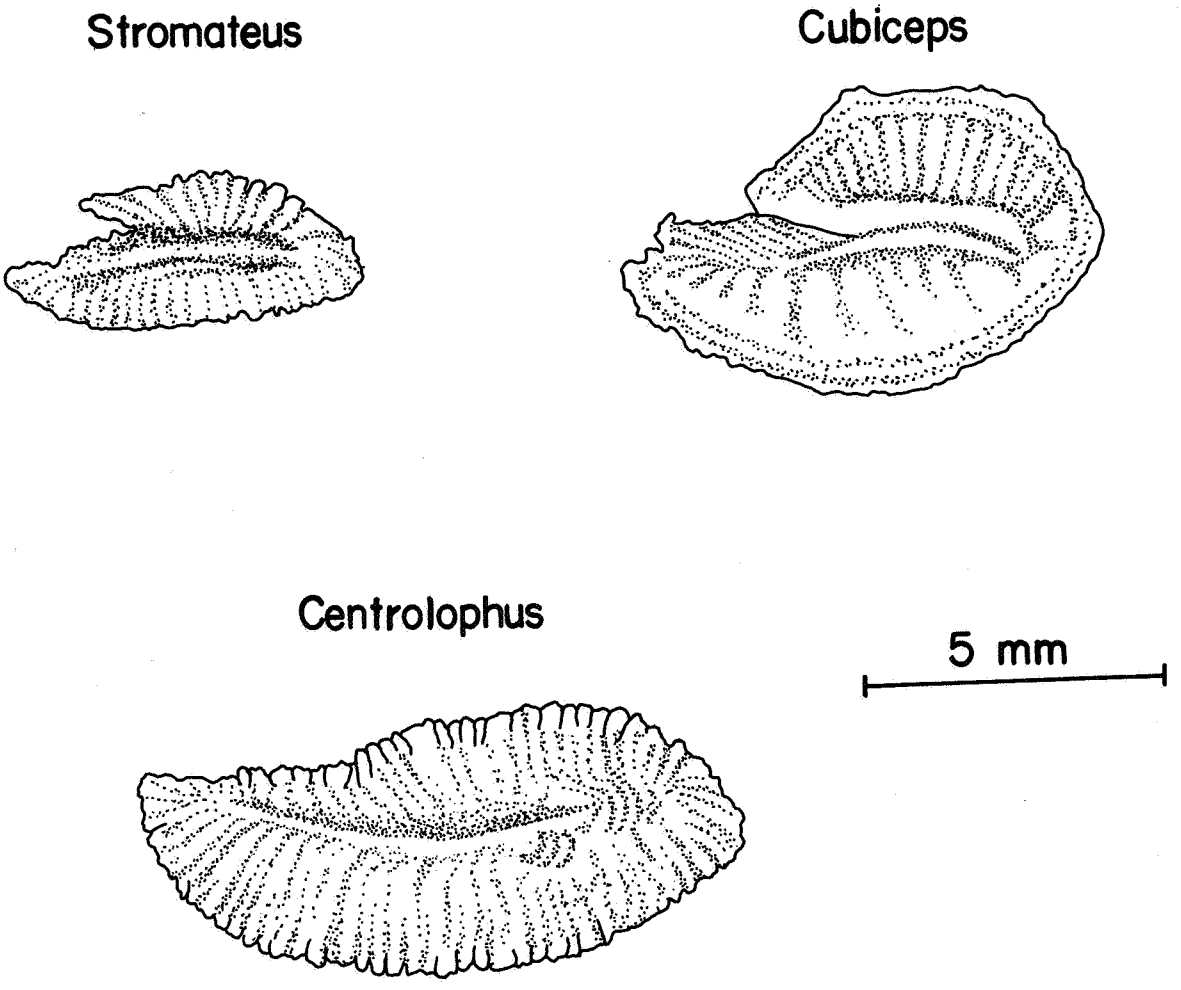

Figure 2

Drawings of three representative otoliths.

Figure 3

Otolith thin-section of Roccus lineatus approximately parallel to the lenticular faces.

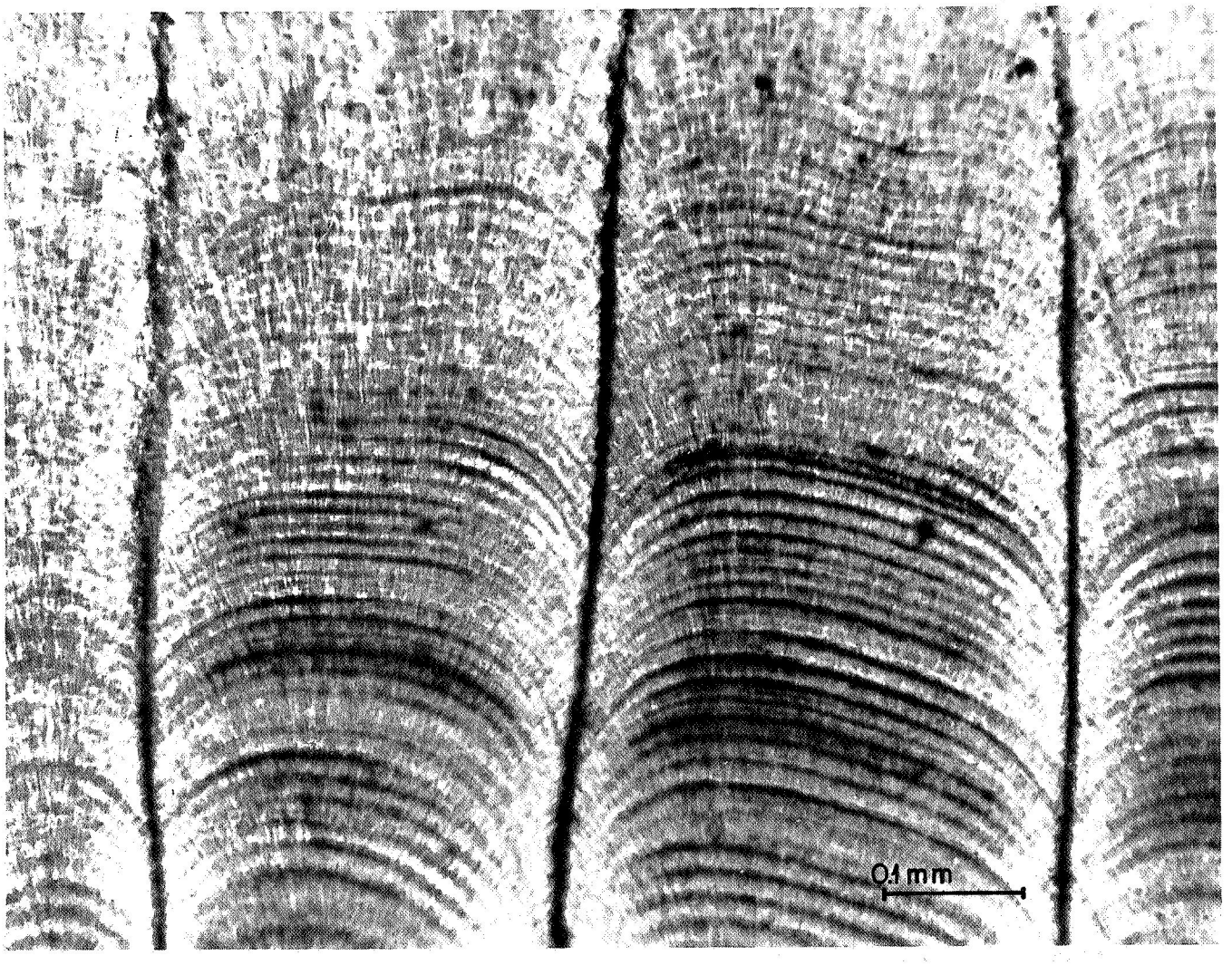

Figure 4

Otolith thin-section of Roccus lineatus approximately parallel to the lenticular faces.

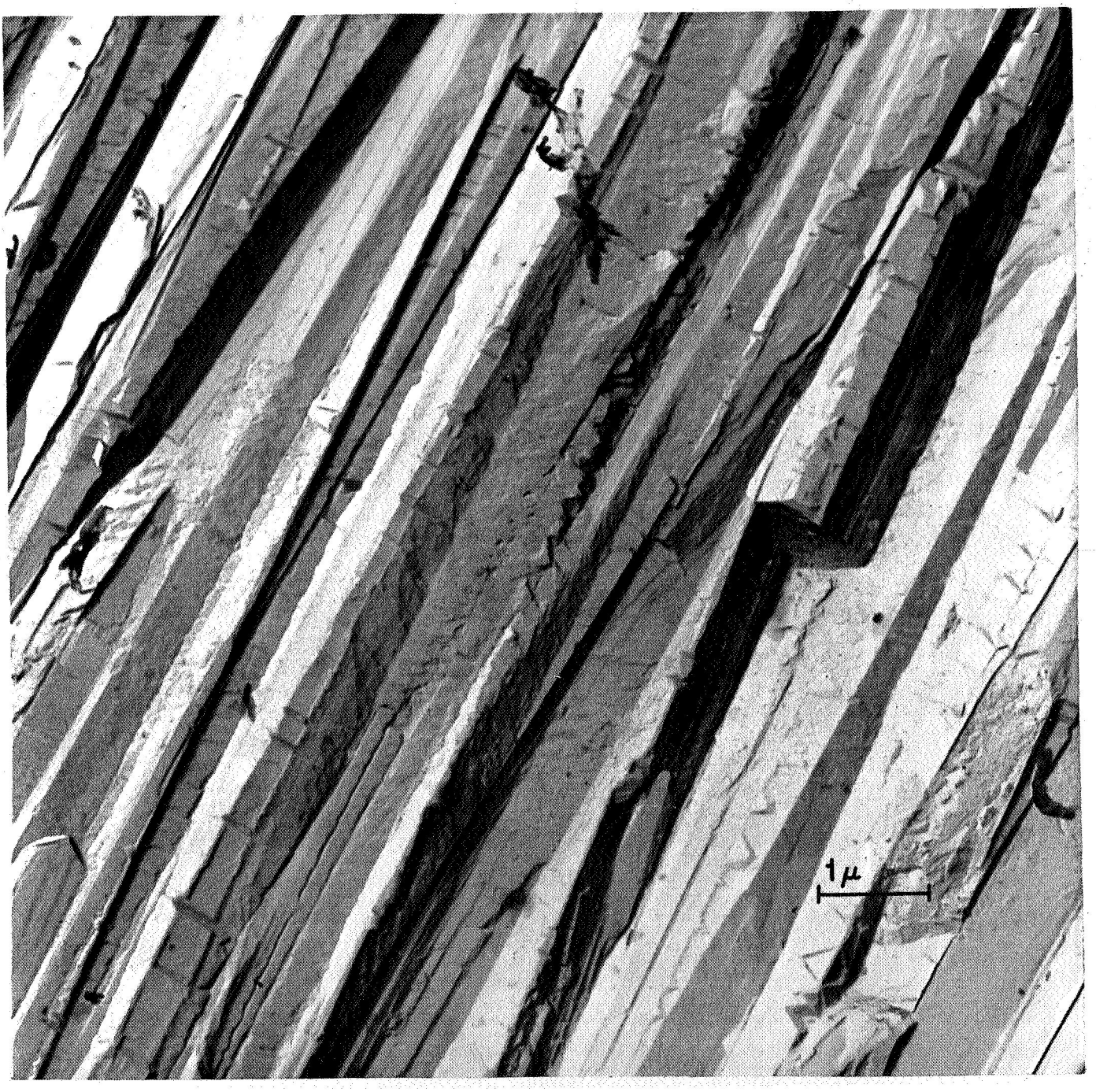

Figure 5

Electronmicrograph of otolith of Aplodinotus grunniens (platinum-carbon replica).

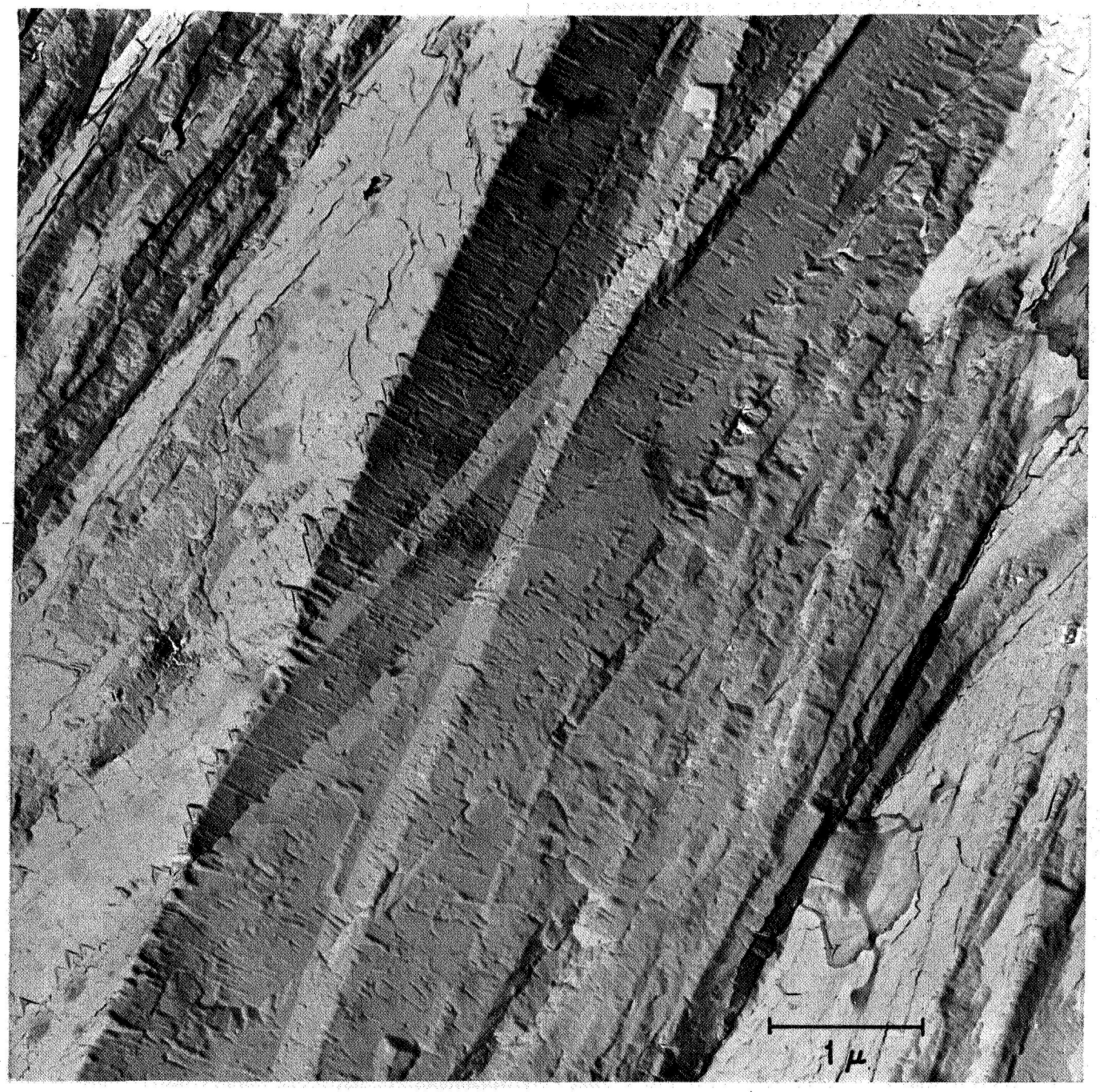

Figure 6

Electronmicrograph of otolith of Roccus lineatus (platinum-carbon replica).

Figure 7

Electronmicrograph of otolith of Roccus lineatus (platinum-carbon replica).

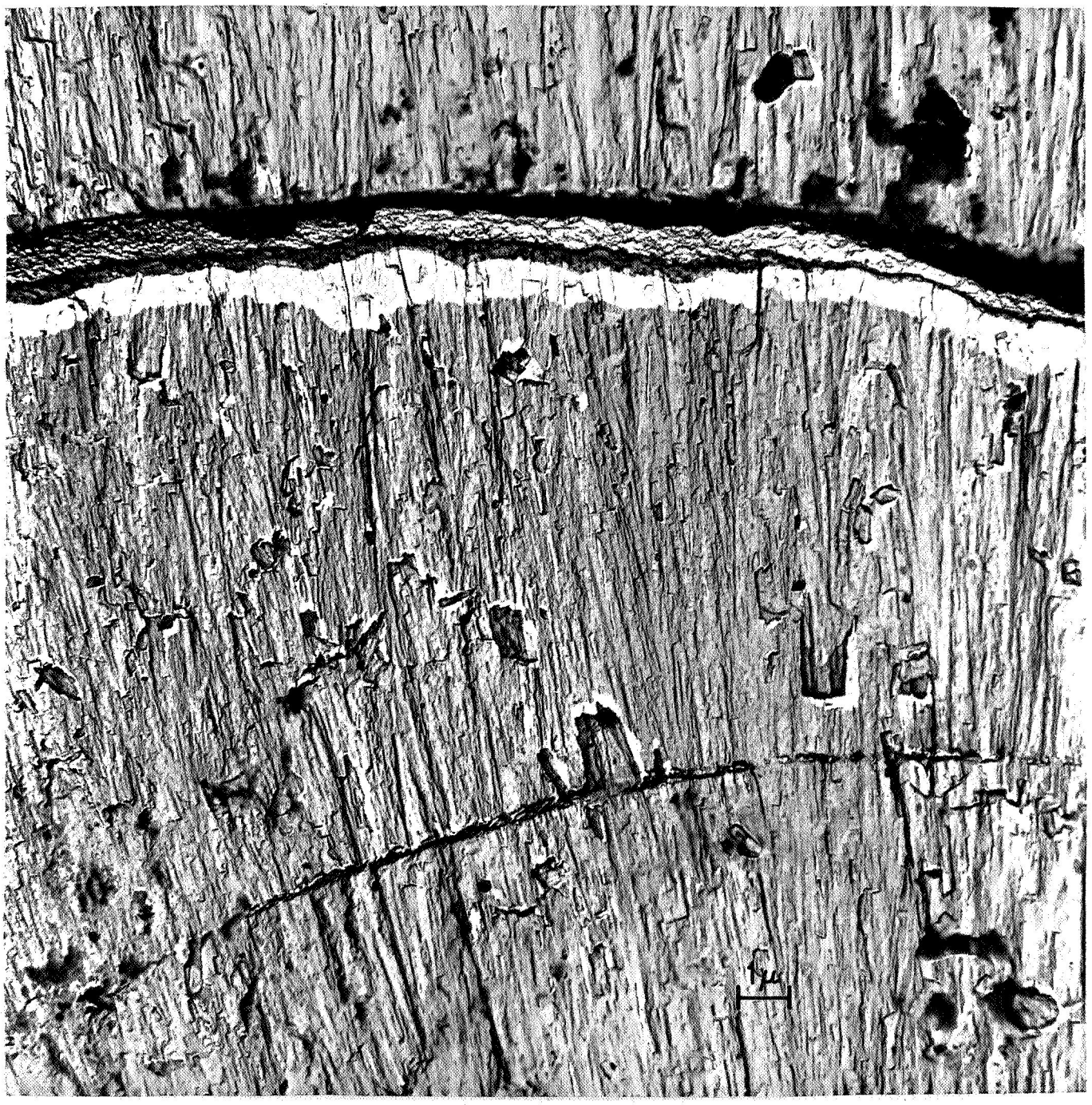

Figure 8

Electronmicrograph of otolith of Aplidonotus grunniens (platinum-carbon replica).

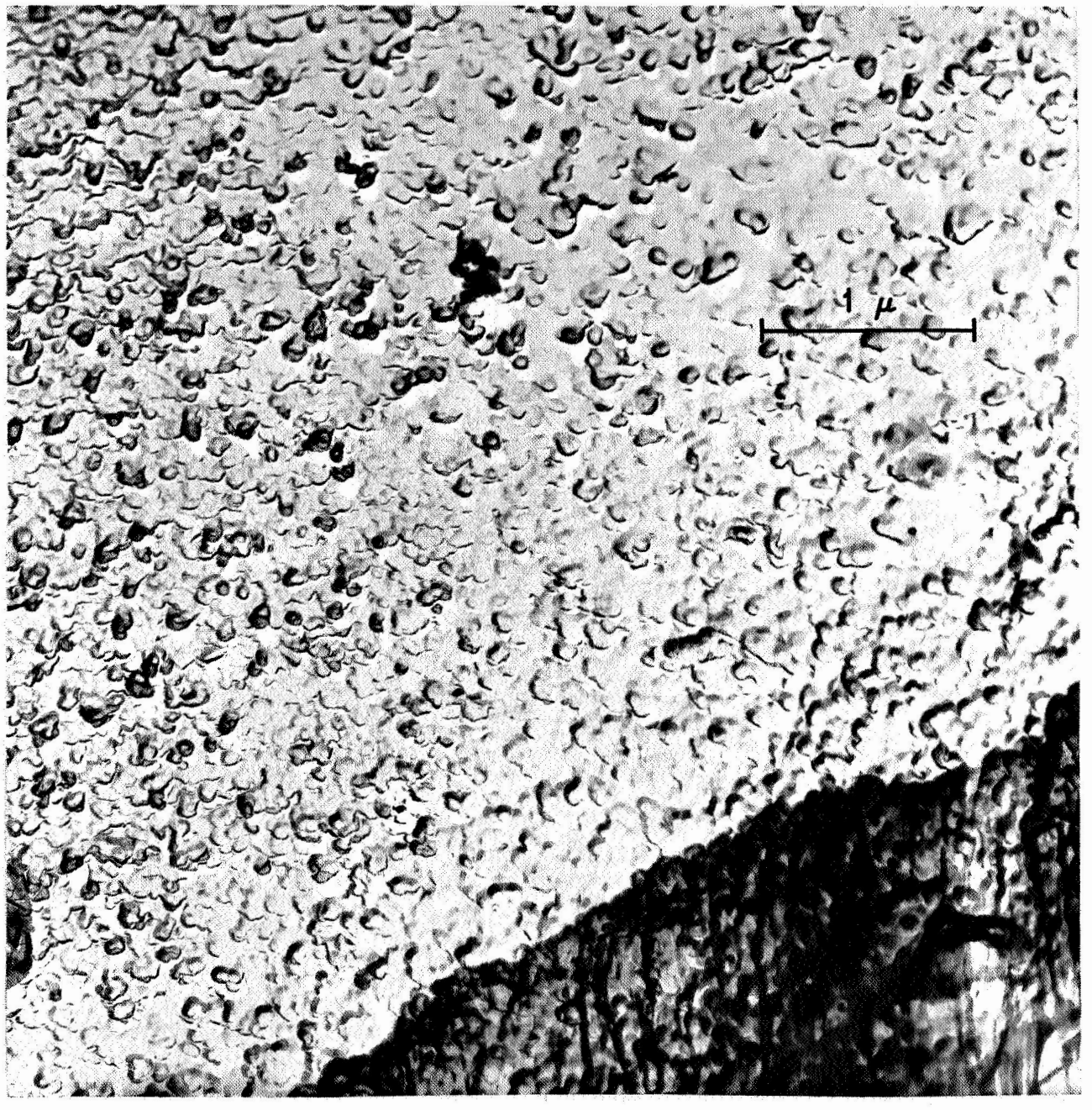

Figure 9

Electronmicrograph of otolith of Aplidonotus grunniens showing the surface structure of the mineralized tissue (platinum-carbon replica).

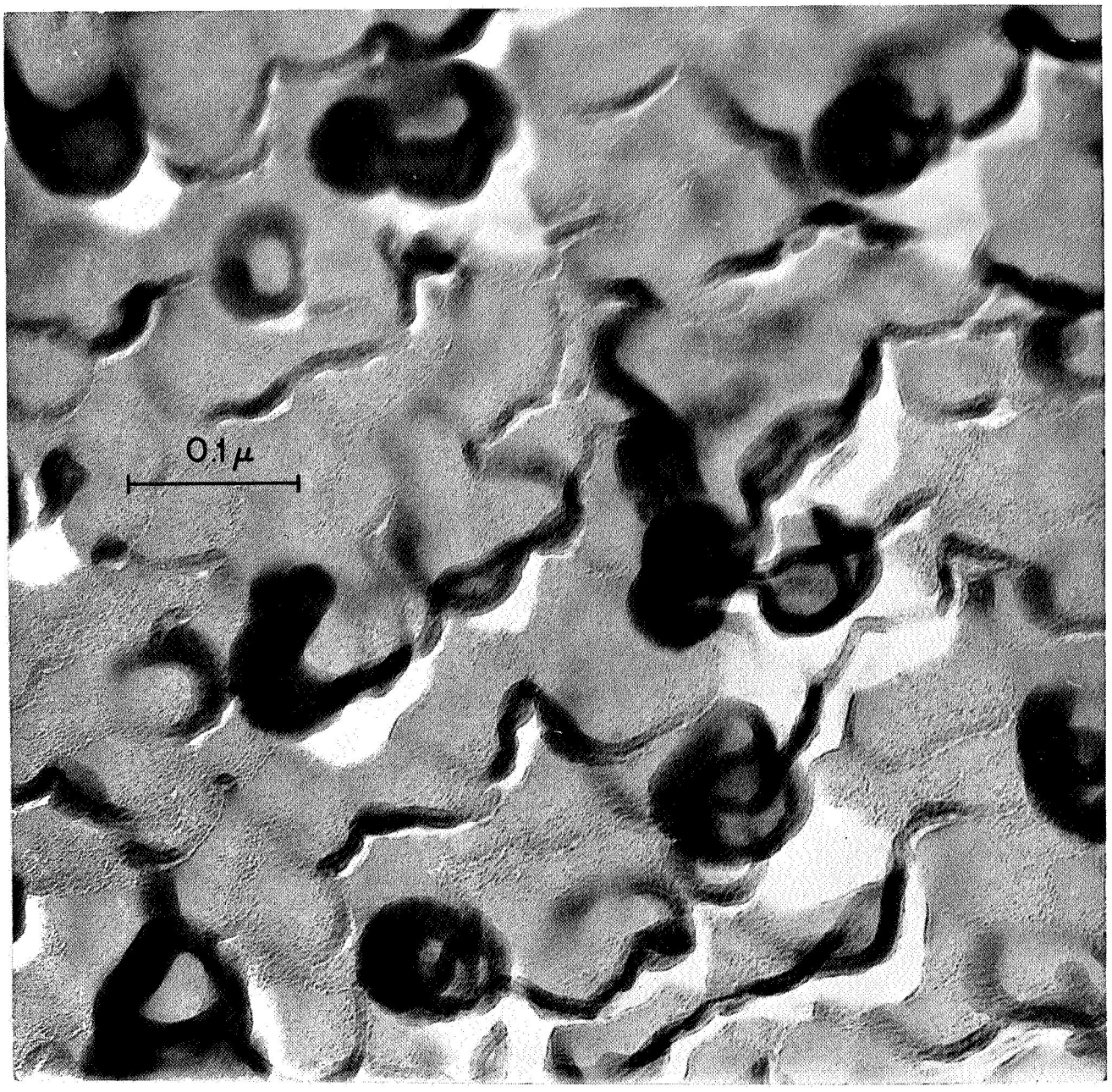

Figure 10

Electronmicrograph of otolith of Aplidonotus grunniens. The protein chains are coiled in a systematic fashion and some structural details of the individual chains are revealed (platinum-carbon replica).

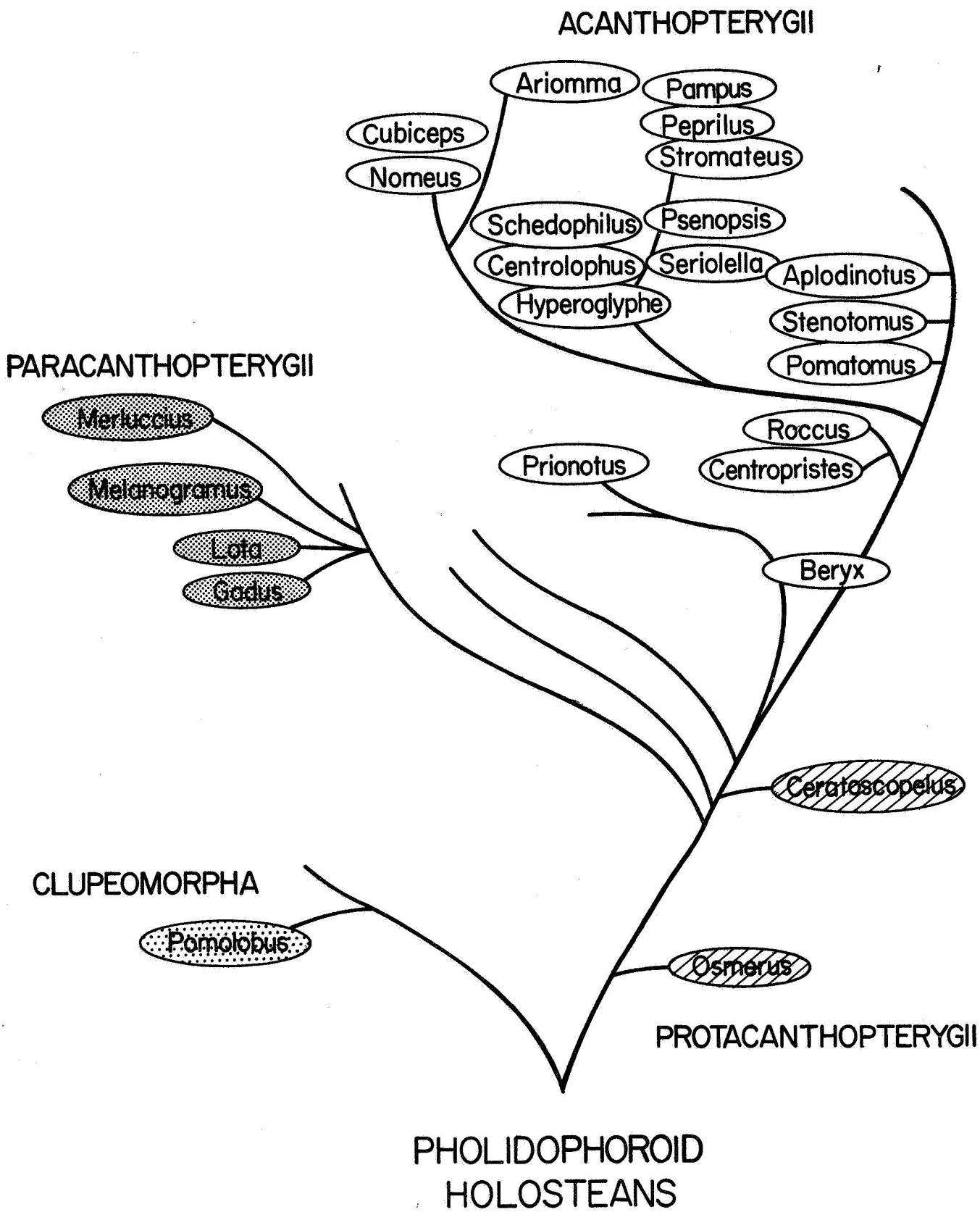

Figure 11

Phylogenetic relationships among species studied in the present report (after Greenwood et al., 1966).